Supplemental Acknowledgements

BRI COVID-19 Research Team

Carolina Acosta Vega (Benaroya Research Institute at Virginia Mason), Pascal Akl (Virginia Mason Medical Center), Kassidy Benoscek (Benaroya Research Institute at Virginia Mason), Anna Bjork (Benaroya Research Institute at Virginia Mason), Ross Christy-Espejo (Benaroya Research Institute at Virginia Mason), Aloisa Jean Vince Cruz (Virginia Mason Medical Center), Donya Derakshani (Benaroya Research Institute at Virginia Mason), Bryce Fuchs (Benaroya Research Institute at Virginia Mason), Nicole Gilbert (Benaroya Research Institute at Virginia Mason), Debbie Gretsch (Virginia Mason Medical Center, Seattle, WA, USA), Nathan Hawley (Benaroya Research Institute at Virginia Mason), Hailee Herbst (Benaroya Research Institute at Virginia Mason), Richard Jaggers (Virginia Mason Medical Center, Seattle, WA, USA), Deric Khuat (Benaroya Research Institute at Virginia Mason), Anna Kus (Benaroya Research Institute at Virginia Mason), Leanne Lewis (Virginia Mason Medical Center), Claire Mangan (Benaroya Research Institute at Virginia Mason), Adarsh Manjunath (Benaroya Research Institute at Virginia Mason), Gina Marchesini (Benaroya Research Institute at Virginia Mason), Pamela Miranda (Benaroya Research Institute at Virginia Mason), Keagan Moo (Benaroya Research Institute at Virginia Mason), Peter Morawski (Benaroya Research Institute at Virginia Mason), , Thien-Son Nguyen (Benaroya Research Institute at Virginia Mason), Adam Ortega (Virginia Mason Medical Center), Tyler Paxton (Virginia Mason Medical Center), Sylvia Posso (Benaroya Research Institute at Virginia Mason), Charlie Quinn (Benaroya Research Institute at Virginia Mason), Paxton Reed (Benaroya Research Institute at Virginia Mason), GeVaughn Royster (Virginia Mason Medical Center), Steven Ruhoy (Virginia Mason Medical Center), Sheila Scheiding (Benaroya Research Institute at Virginia Mason), Leslie Stevens (Benaroya Research

Institute at Virginia Mason), Punam Verma (Virginia Mason Medical Center), Alex Walker (Benaroya Research Institute at Virginia Mason), Alice Wiedeman (Benaroya Research Institute at Virginia Mason), Kyle Williams (Benaroya Research Institute at Virginia Mason), Cameron Willman (Benaroya Research Institute at Virginia Mason).

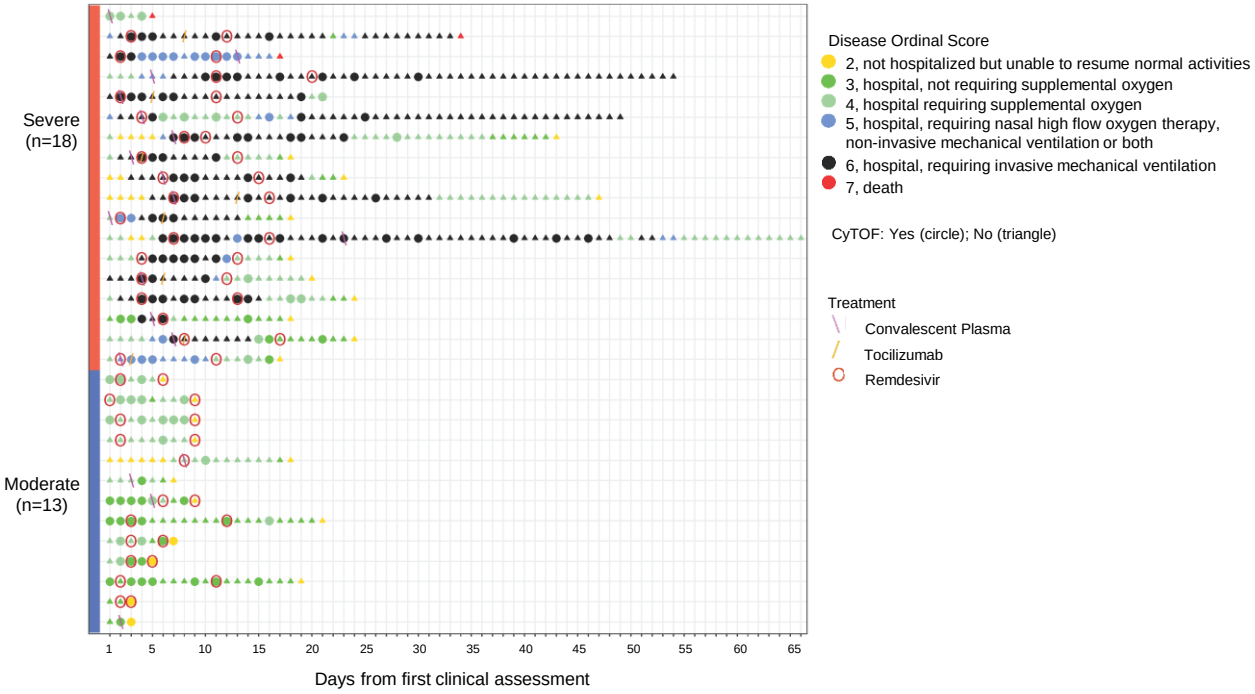

Supplemental Figure 1. Clinical course, mechanistic data and treatments for COVID-19 subjects. Subset of COVID-19 cohort that were treated with remdesivir, tocilizumab and/or convalescent plasma (n=13 for moderate COVID-19, and n=18 for severe COVID-19). Each subject is represented in one row. X-axis: days from first clinical assessment, typically the date of hospital admission. Colored points represent the ordinal score captured daily. Dates with CyTOF data available are denoted by circles; dates without CyTOF data are denoted by triangles. Treatments indicated are convalescent plasma (pink backslash), tocilizumab (yellow forward slash) and remdesivir (red open circles).

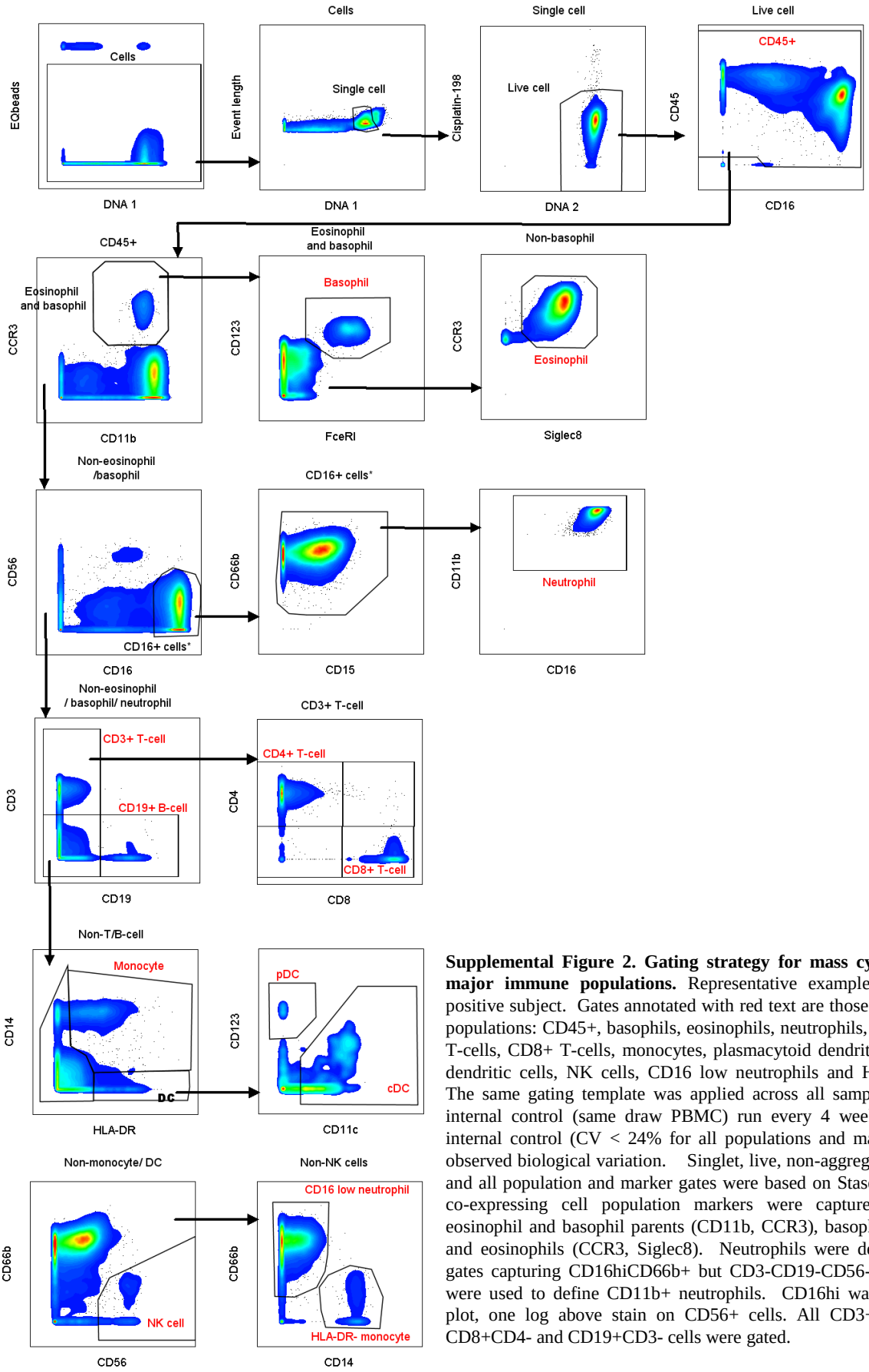

Supplemental Figure 2. Gating strategy for mass cytometry analysis of major immune populations. Representative example from a COVID-19 positive subject. Gates annotated with red text are those defining the reported populations: CD45+, basophils, eosinophils, neutrophils, CD3+ T-cells, CD4+ T-cells, CD8+ T-cells, monocytes, plasmacytoid dendritic cells, conventional dendritic cells, NK cells, CD16 low neutrophils and HLA-DR- monocytes. The same gating template was applied across all samples in addition to an internal control (same draw PBMC) run every 4 weeks. Variation for the internal control (CV < 24% for all populations and markers) was less than observed biological variation. Singlet, live, non-aggregate gates are standard and all population and marker gates were based on Staser et.al (31). All cells co-expressing cell population markers were captured in the gates for eosinophil and basophil parents (CD11b, CCR3), basophils (CD123, FceR1), and eosinophils (CCR3, Siglec8). Neutrophils were defined using Boolean gates capturing CD16hiCD66b+ but CD3-CD19-CD56- and HLA-DR- cells were used to define CD11b+ neutrophils. CD16hi was defined by contour plot, one log above stain on CD56+ cells. All CD3+CD19-, CD4+CD8-, CD8+CD4- and CD19+CD3- cells were gated.

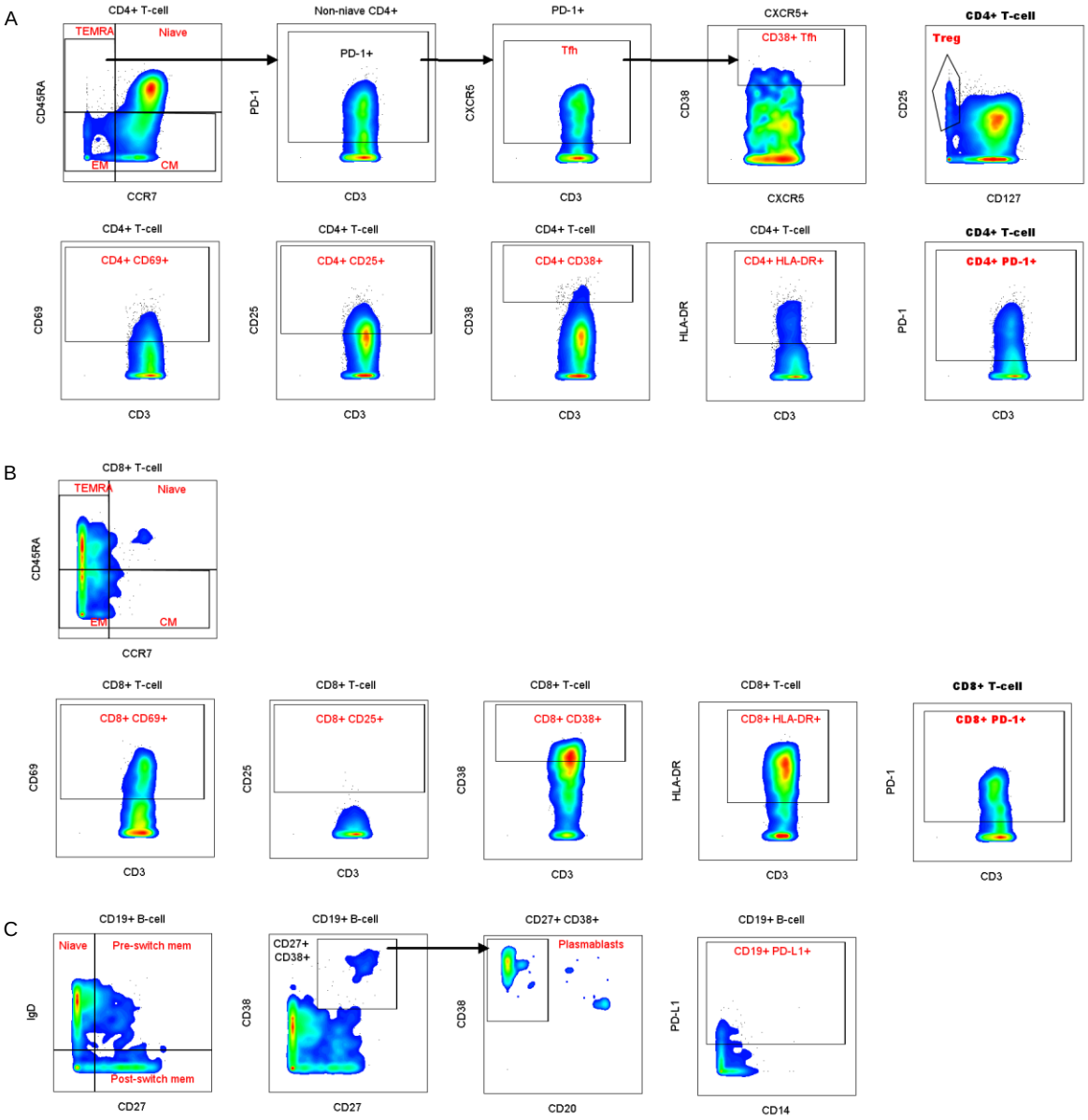

Supplemental Figure 3. Gating strategy for mass cytometry analysis of T-cell and B-cell subsets. Representative example from a COVID-19 positive subject. Gates annotated with red text are those defining the reported populations. (**A**) Characterization of CD4+ T-cell subsets and activation. (**B**) Characterization of CD8+ T-cell subsets and activation. (**C**) Characterization of B-cell subsets and activation. The same gating template was applied across all samples based on Staser et.al (31). CCR7xCD45RA quadrant gates for CD3+ CD4 T cells were set based on a tight gate on the naive CCR7+CD45RA+ population. This gate was applied to CD8 T cells. PD-1, CXCR5, CD38, HLA-DR, CD69, and CD25 gates were based on naive cells of controls that lacked expression of these markers and were never adjusted when applying to study samples. CD27xIgD quadrant gates for CD19+ B cells were set based on the naive IgD+CD27- population. PDL-1 was based on a negative control and was never adjusted when applying to study samples. To determine gates for activation markers such as CD25, CD69 and CD38 on T cells and PD-L1 on myeloid cells, we first analyzed 12 samples from 6 subjects with moderate COVID-19 and 6 subjects with severe COVID-19. Gates were set based on a comparison between samples that were clearly highly activated and those that were clearly non-activated. These gates were then applied to all samples in the study and used consistently for all populations analyzed. Specifically, gates for CD25, CD38, CD69, HLA-DR, PD-1 and PD-L1 were the same for all cell types where they were applied.

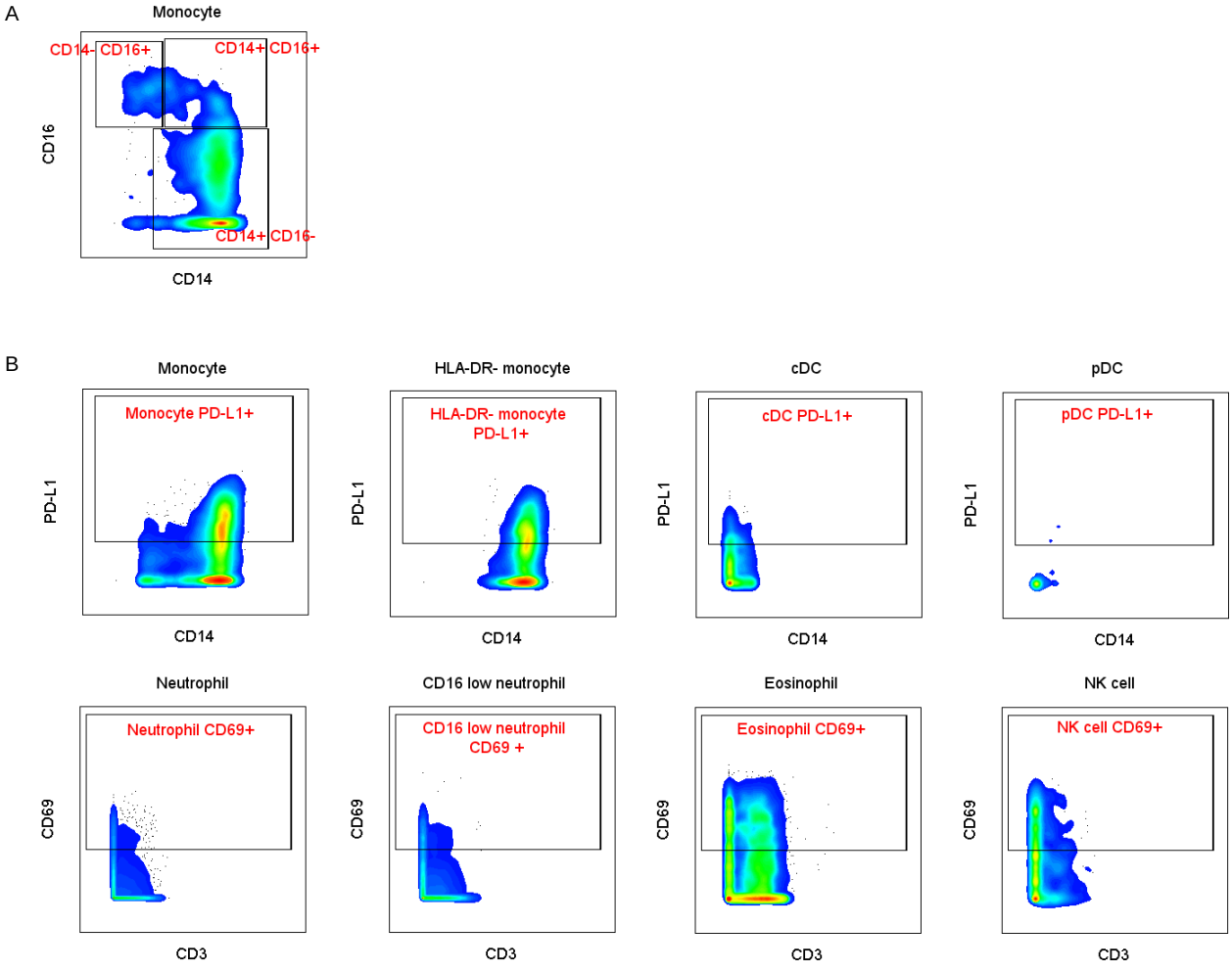

Supplemental Figure 4. Gating strategy for mass cytometry analysis of monocyte, dendritic cell, neutrophil, eosinophil and NK cell subsets. Representative example from a COVID-19 positive subject. Gates annotated with red text are those defining the reported populations. (**A**) Characterization of classical (CD14+CD16-), non-classical (CD14loCD16+) and intermediate (CD14+CD16+) monocyte subsets. Gating strategy for these subsets removed cells expressing CCR3, CD15, CD66b, CD3, CD19 and CD56 to define the parent monocyte population. (**B**) Characterization of PD-L1 and CD69 expression by monocytes, dendritic cells, neutrophils, eosinophils and NK cells. Populations were gated as in Supplemental Figures 2 and 3.

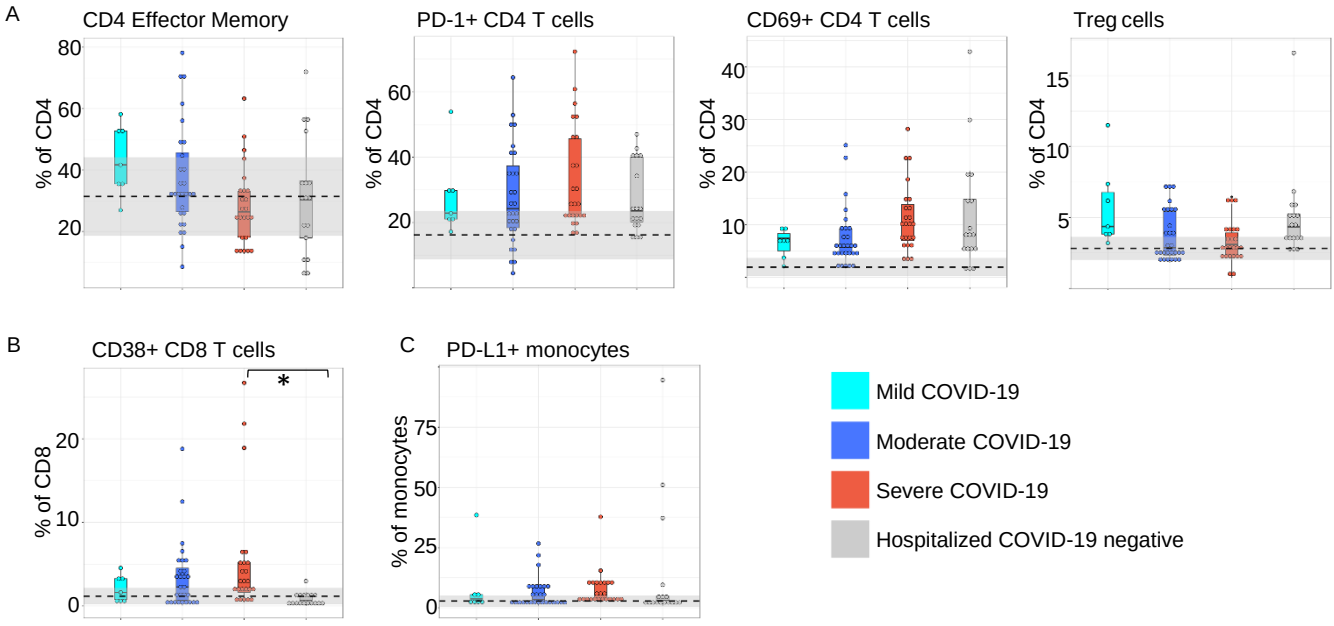

Supplemental Figure 5. Relative proportions of immune cell sub-types vary by disease severity. Shown are CyTOF cell frequencies expressed as percentage of parent population. (**A**) CD4 T cell subsets, (**B**) CD8 T cell subset, and (**C**) Monocytes

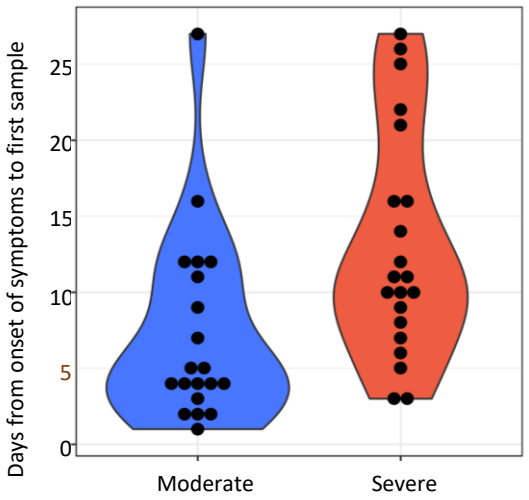

Supplemental Figure 6. Sample collection dates relative to the onset of symptoms for moderate and severe COVID-19 subjects with unambiguous onset dates.

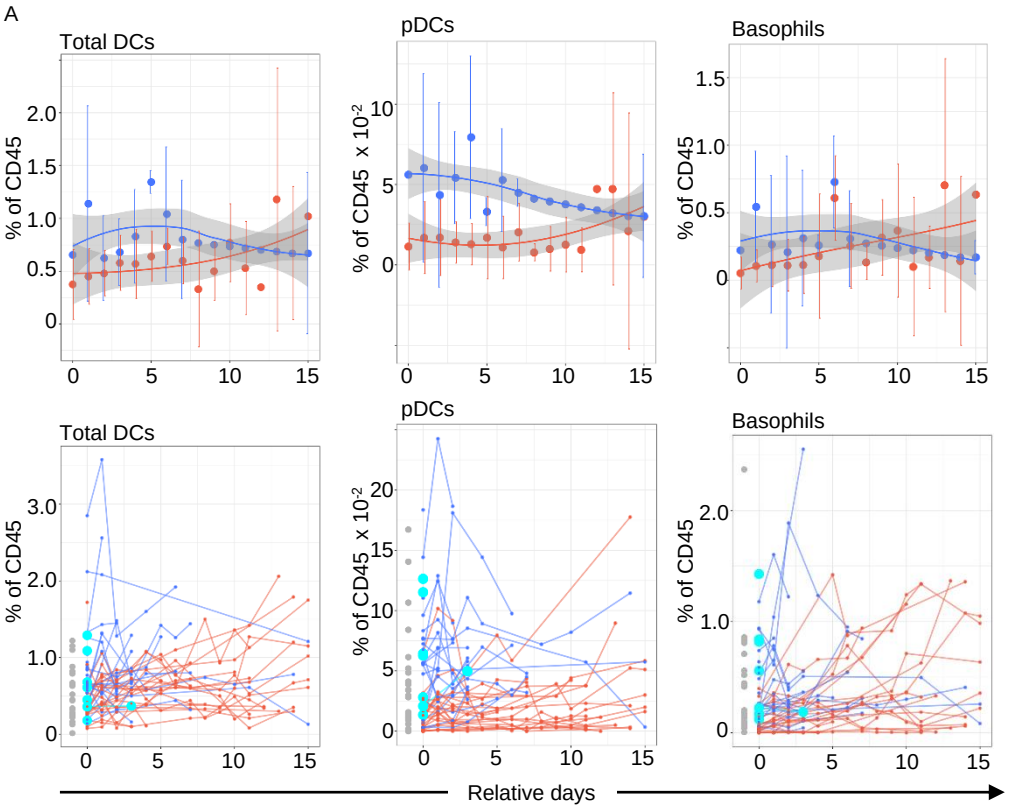

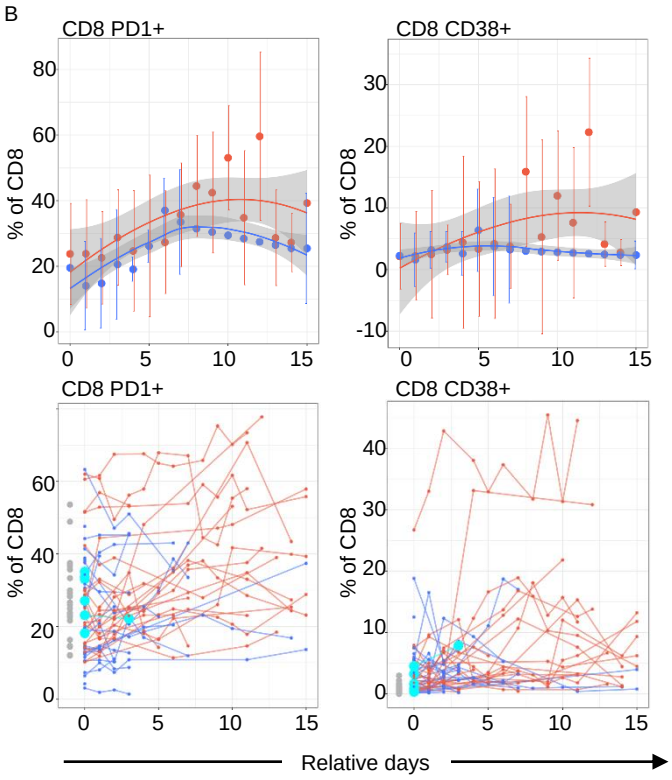

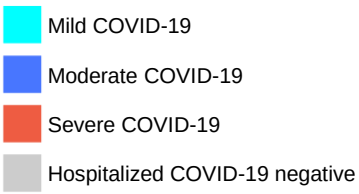

Supplemental Figure 7. Smoothed-average, and per-patient longitudinal sampling of immune cell populations measured as percentage of CD45+ cells (**A**) and percentage of CD8+ cells (**B**). The horizontal axes indicate the number of days from first hospitalization. The upper panels in **A** and **B** show smoothed, average trajectories per patient group (see color key). Loess trajectory smoothing was performed on the median values (colored disks) for each group at each time point. Vertical bars indicate +/- 1 standard deviation around the median at each time point. Plot points without vertical error bars are from single data points, or interpolated values used for smoothing. The lower panels show the raw (un-smoothed) trajectories per donor colored by patient group. For comparison, corresponding values for hospitalized COVID-19-negative patients (gray dots) and for patients with mild Covid-19 (cyan dots) are shown on the left-hand side of each panel.

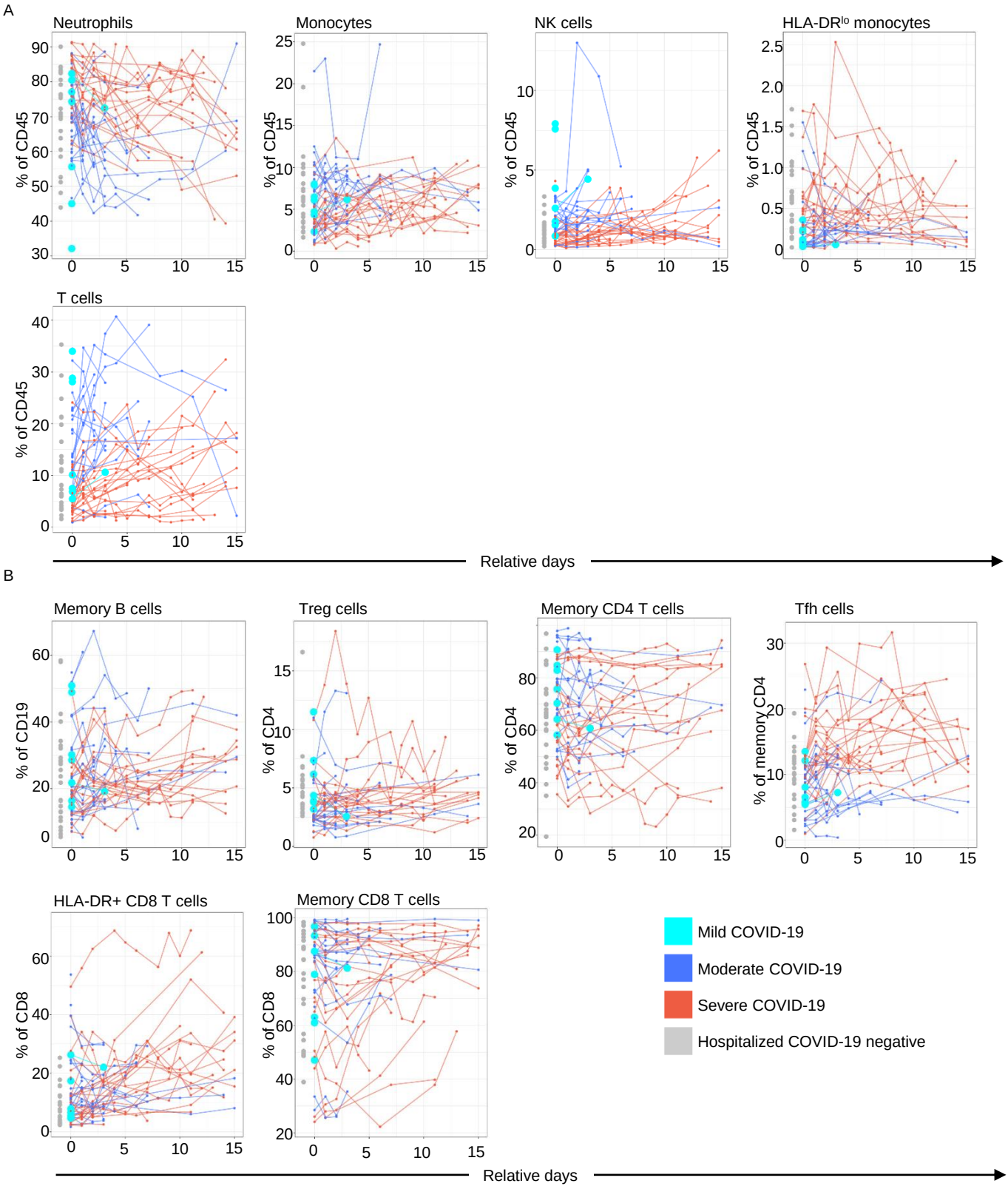

Supplemental Figure 8. Longitudinal sampling for individuals and smoothed averages for populations as percentages of CD45 (**A**) and indicated parent populations (**B**). Days (relative) from first hospitalization are shown. Loess trajectory smoothing was performed on the median values (colored disks) for each group at each time point. Vertical bars indicate +/- 1 standard deviation around the median at each time point. Plot points without vertical error bars are from single data points, or interpolated values used for smoothing.

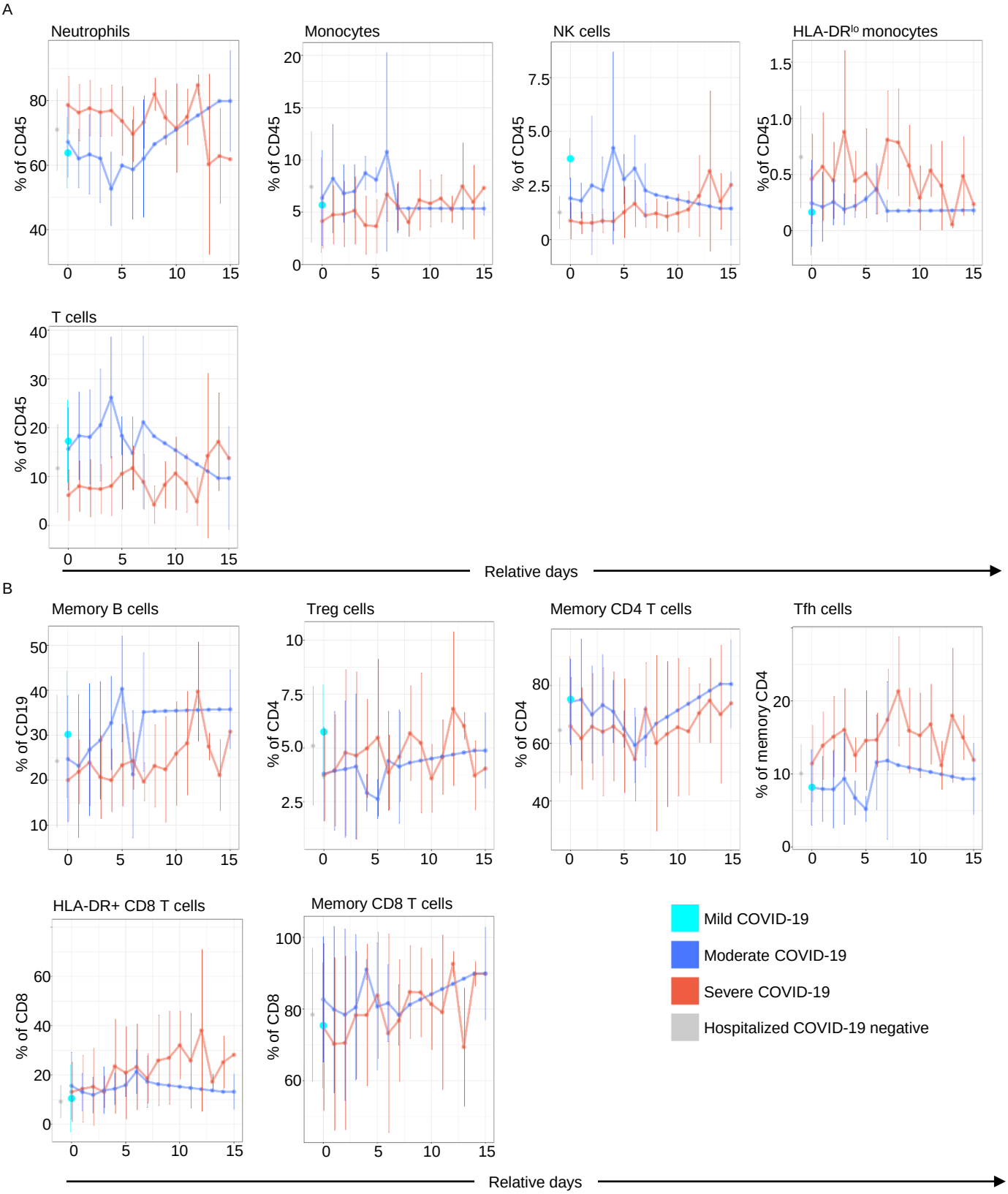

Supplemental Figure 9. Un-smoothed time-trajectories of median cell frequencies per patient group for the same cell populations as in Supplemental Figures 8A and 8B.

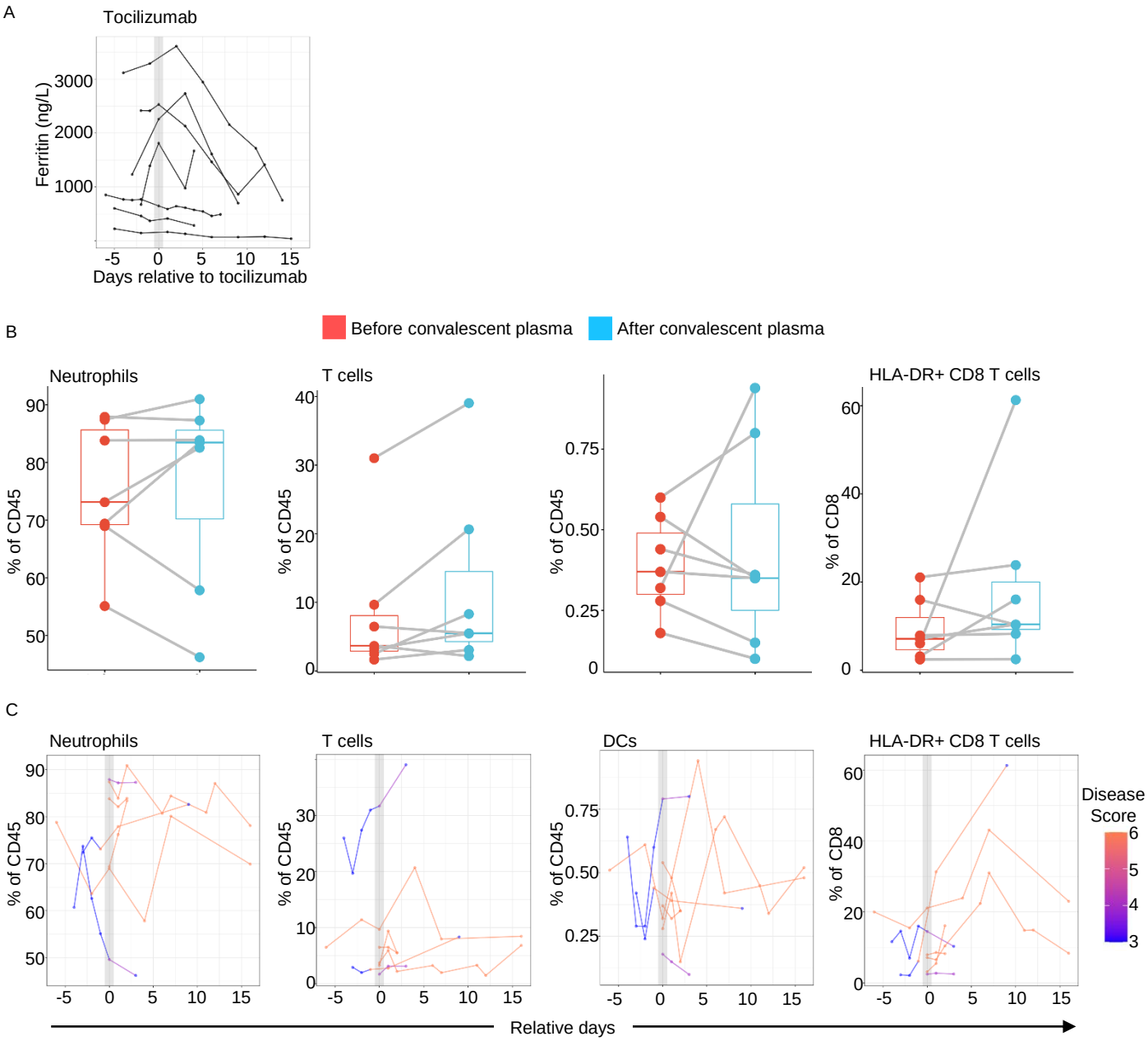

Supplemental Fig. 10. Analysis of clinical and immune parameters after Tocilizumab and convalescent plasma treatment. (**A**) Serum Ferritin in patients receiving Tociluzimab. Each line represents an individual patient. (**B**) Plots showing the percent of the indicated populations in convalescent plasma-treated patients before and after treatment, using the same time points used for analysis in Figure 7C see Supplemental Table 3. None of the changes were significant. (**C**) Plots showing all the data points available for convalescent plasma treated patients for the indicated populations shown in (B). Each line represents an individual patient and the color of the line reflects the clinical ordinal score at the time of sampling. Populations were chosen to match those in Figure 10D and 10E.

Supplemental Table 1. CyTOF panel antibodies

Label	Target	Clone	Catalog #	Supplier
89Y	CD45	HI30	3089003B	Fluidigm
141Pr	CD3	UCHT1	3141019B	Fluidigm
142Nd	CD19	HIB19	3142001B	Fluidigm
143Nd	CD123	6H6	3143014B	Fluidigm
144Nd	CD15	W6D3	3144019B	Fluidigm
145Nd	CD4	RPA-T4	3145001B	Biolegend
146Nd	IgD	IA6-2	3146005B	Fluidigm
147Sm	CD11c	Bu15	3147008B	Fluidigm
148Nd	FceR1	AER-37[CRA-1]	334602	Biolegend
149Sm	CD127	A019D5	3149011B	Fluidigm
150Nd	CD27	LG.3A10	3150017B	Fluidigm
151Eu	CCR7	G043H7	353202	Biolegend
152Sm	CD11b	LH2	393102	Biolegend
153Eu	HLA-DR	L243	307602	Biolegend
154Sm	CD38	HB-7	356602	Biolegend
155Gd	PD-1	EH12.2H7	3155009B	Fluidigm
156Gd	PD-L1	29E.2A3	3156026B	Fluidigm
158Gd	Siglec 8	7C9	347102	Biolegend
159Tb	CCR3	5E8	310702	Biolegend
160Gd	CD14	M5E2	3160001B	Fluidigm
161Dy	CD56	NCAM16.2	559043	BD
162Dy	CD66b	80H3	3162023B	Fluidigm
164Dy	CXCR5	RF8B2	3164029B	Fluidigm
165Ho	CD45RA	HI100	304102	Biolegend
166Er	CD24	ML5	3166007B	Fluidigm
167Er	CD8	RPA-T8	301002	Biolegend
169Tm	CD25	2A3	3169003B	Fluidigm
170Er	CD69	FN50	310902	Biolegend
171Yb	CD141	M80	344102	Biolegend
172Yb	CD20	2H7	302302	Biolegend
175Lu	HLA-A2	BB7.2	343302	Biolegend
176Yb	HLA-B7	BB7.1	372402	Biolegend
209Bi	CD16	3G8	3209002B	Fluidigm

Supplemental Table 2. Treatment cohorts demographic and clinical characteristics

	Tocilizumab (n=7)	Convalescent plasma (n= 7)
	Median (Range)	**Median (Range)**
Age (yrs)	55 (43-63)	63 (42-85)
Number of Days Hospitalized	18 (11-40)	20 (4-60)
BMI	29.8 (26.8-48.9)	30.4 (18.1-48.9)
Disease score at time of experimental treatment	6 (5-6)	6 (4-6)
Pre-treatment CRP (mg/L)	285.3 (174.6-350.2)	215.9 (27.8-323.9)
Pre-treatment ferritin (ng/mL)	1811 (144-3290)	330 (173-732)
Pre-treatment Soluble IL-6 (pg/mL)	323 (99-1490)	1032 (51-51512)
	# (%)	**# (%)**
Received care in critical care unit (CCU)	7 (100%)	5 (71.4%)
Outcome: discharged	6 (85.7%)	6 (85.7%)
Outcome: deceased	1 (14.3%)	1 (14.3%)
Female	5 (71.4%)	3 (42.9%)
Race		
Asian	1 (14.3%)	0 (0%)
White	1 (14.3%)	5 (71.4%)
Unknown/Other	5 (71.4%)	2 (28.6%)
Ethnicity: Hispanic/Latino	4 (57.1%)	2 (28.6%)
Exposure to experimental medicine (ever)		
Hydroxychloroquine	1 (14.3%)	1 (14.3%)
Remdesivir	7 (100%)	6 (85.7%)
Tocilizumab	7 (100%)	2 (28.6%)
Convalescent Plasma	6 (85.7%)	7 (100%)

Supplemental Table 3. Time points analyzed in Figure 10 and Supplemental Figure 10

Tocilizumab cohort	Pre-treatment time point (days)	Post-treatment time point (days)
Patient #1	-1	7
Patient #2	0	2
Patient #3	-4	5
Patient #4	-1	4
Patient #5	0	2
Patient #6	-1	2
Patient #7	-3	3
Convalescent plasma cohort		
Patient #1	0	2
Patient #2	0	4
Patient #3	-1	3
Patient #4	-1	9
Patient #5	0	3
Patient #6	0	2
Patient #7	0	2